



Unsupervised Spike Sorting of extracellular electrophysiological recording in subthalamic nucleus of Parkinsonian patients

Olga K. Chibirova^{a,*}, Tetyana I. Aksenova^{a,b}, Alim-Louis Benabid^{a,c}, Stephan Chabardes^a, Steeve Larouche^d, Jean Rouat^d, Alessandro E.P. Villa^{a,c}

^a *Laboratory of Preclinical Neuroscience; INSERM U318; CHUG Michallon Pavillon B; BP 217; F-38043 Grenoble Cedex 9; France*

^b *Institute of Applied System Analysis; Ukrainian Academy of Sciences; Prospekt Peremogy; 37; Kyiv 03056; Ukraine*

^c *Laboratoire de Neurobiophysique; Université Joseph Fourier Grenoble 1; UFR Médecine CHUG Michallon Pavillon B; BP 217; F-38043 Grenoble Cedex 9; France*

^d *Département de génie électronique et de génie informatique; IMSI; Université de Sherbrooke 2500 boul. de l'Université; Sherbrooke; Que.; Canada J1K 2R1*

Abstract

The present study demonstrates the application of the Unsupervised Spike Sorting algorithm (USS) to separation of multi-unit recordings and investigation of neuronal activity patterns in the subthalamic nucleus (STN). This nucleus is the main target for deep brain stimulation (DBS) in Parkinsonian patients. The USS comprises a fast unsupervised learning procedure and allows sorting of multiple single units, if any, out of a bioelectric signal. The algorithm was tested on a simulated signal with different levels of noise and with application of Time and Spatial Adaptation (TSA) algorithm for denoising. The results of the test showed a good quality of spike separation and allow its application to investigation of neuronal activity patterns in a medical application. One hundred twenty-four single channel multi-unit records from STN of 6 Parkinsonian patients were separated with USS into 492 single unit trains. Auto- and crosscorrellograms for each unit were analyzed in order to reveal oscillatory, bursting and synchronized activity patterns. We analyzed separately two brain hemispheres. For each hemisphere the percentage of units of each activity pattern were calculated. The results were compared for the first and the second operated hemispheres of each patient and in total. © 2004 Elsevier Ireland Ltd. All rights reserved.

Keywords: Spike sorting; Neuronal activity patterns; Basal ganglia; STN; Parkinson's disease

* Corresponding author.

E-mail addresses: Olga.Chibirova@ujf-grenoble.fr (O.K. Chibirova); Tatyana.Aksyonova@ujf-grenoble.fr (T.I. Aksenova); Alim-Louis.Benabid@ujf-grenoble.fr (A.-L. Benabid); SChabardes@chu-grenoble.fr (S. Chabardes); slarouche@hermes.usherb.ca (S. Larouche); Jean.Rouat@ieee.org (J. Rouat); Alessandro.Villa@ujf-grenoble.fr (A.E.P. Villa)

1. Introduction

Models of basal ganglia dysfunctions are used to explain the pathophysiological symptoms that characterize Parkinson's Disease (PD). The validity of such models rests upon the correlation between the neuronal activity in the basal ganglia and the degree of clinical symptoms due to PD (Asai et al., 2003; Abe et al., 2003; Niktarash, 2003). The subthalamic nucleus (STN) plays a key role in the regulation of the output pathway of basal ganglia. The inactivation of STN in patients affected by PD dramatically reduces much of the clinical symptoms and its reversible inactivation by deep brain stimulation (DBS) is one of most valuable techniques of present functional neurosurgery (Benabid et al., 1994; Limousin et al., 1998).

The investigation of the activity patterns of subthalamic neurons (Magarinos-Ascone et al., 2000; Liu et al., 2002) represents an important objective for better understanding the mechanisms that subserve the regulatory loops of the basal ganglia. High and low-frequency oscillatory patterns in basal ganglia and their modifications in response to behavioral events have been recently studied (Cassidy et al., 2002; Bevan et al., 2002; Levy et al., 2002b). It has been proposed that an increase in synchronization between neuronal discharges in the basal ganglia contributes to generate the appearance of several clinical symptoms typical of PD. Synchronization of the activity patterns (Levy et al., 2000, 2002) and tremor-related neuronal firing (Rodrigues et al., 1998; Hurtado et al., 1999; Hutchison et al., 1997) were examined for Parkinsonian patients. Changes of neuronal firing patterns have been associated to improvement of clinical symptoms typical of PD during DBS (Benazzouz et al., 2000; Hashimoto et al., 2003).

During surgery the electrophysiological signal recorded by the microelectrodes introduced in the basal ganglia always includes background activity and an undetermined amount of noise. Separation of the signals of interest corresponding to single units discharges is essential for recording spike trains. In the present study we demonstrate the application of an unsupervised method for spike sorting to separate spike trains (Aksenova et al., 2003). We present new tests applied for the assessment of this method using a simulated signal with different levels of noise and with denoising by means of TSA (Bahoura and Rouat, 2001).

2. Methods

The Unsupervised Spike Sorting (USS) belongs to the wide class of template matching algorithms for spike sorting. Among different methods used in neurophysiology for spike sorting (Schmidt, 1984; Lewicki, 1998) template matching has become one of the most popular. This technique is based on construction of templates that represent the typical waveform of neuron (Bergman and DeLong, 1992; Forster and Handwerker, 1995; Gadikie and Albus, 1995). The algorithms of this class compare the candidates spike waveforms with all available templates and select the best matching one.

Most of the algorithms construct the templates and compare segments of the signal in time domain. The drawback of this method is that spike waveforms could be slightly distorted not only in amplitude, but also along the time axis. As a consequence, classes of spikes may not form clusters in the feature space related to time domain and the distributions inside the classes may not be Gaussian (Fee et al., 1996). Supervision by a human expert is required for a correct classification.

The method used for spike sorting in USS was described in details in Aksenova et al. (2003, 2002). In this section we present only a short description of the model and the algorithm. We present also the software implementation of the method.

2.1. Model

The method is based on the assumption that neuronal activity may be modeled by a nonlinear oscillating process and spike waveforms can be considered as solutions of an ordinary differential equation with perturbation:

$$\frac{d^n x}{dt^n} = f \left(x, \dots, \frac{d^{n-1} x}{dt^{n-1}} \right) + F(x, \dots, t). \quad (1)$$

The differential equation without perturbation describes a self-oscillating system with a stable limit cycle and the perturbation function $F(x, \dots, t)$ characterizes the signal distortions in both amplitude and phase.

The spikes are considered as trajectories of an ordinary differential Eq. (1) in the phase space with coordinates: $x_1 = x, x_2 = \frac{dx}{dt}, \dots, x_n = \frac{d^{n-1}x}{dt^{n-1}}$. In the assumption that the perturbation function $F(x, \dots, t)$ from the Eq. (1) is bounded by a small value the trajec-

tories stay in the neighborhood of the limit cycle and they are similar one to another. Moreover, if the perturbation function represents a random process with zero mean and small correlation time the trajectories have an asymptotically normal distribution in phase space (Gudzenko, 1962).

We assume that the activity of each neuron is described by its own dynamic Eq. (1), such that the single-unit spikes can be recognized according to their differential equation. In this case trajectories of a single-unit have an asymptotically normal distribution in phase space (Gudzenko, 1962). This means that for the mixture of spikes corresponding to a multi-unit recording the problem of unit separation may be reduced to the problem of separation of mixture of asymptotically normal distributions. The coordinates of the trajectories in phase space were considered as features for spike classification.

2.2. USS algorithm

The algorithm consists of the following stages: (1) extracting spikes from the signal and estimation of its trajectory in phase space; (2) unsupervised iterative learning procedure; (3) on-line classification.

2.2.1. Extracting spikes from the signal and estimation of its trajectory in phase space

The estimation of trajectories in phase space requires calculation of signal derivatives of the original electrophysiological signal. Higher-order derivatives of the signal should be calculated in presence of noise that seriously affects the calculations. For the derivative estimation the following operator was used:

$$D_{\alpha}^k x(t) = \int_R \omega_{\alpha}^k(\tau - t)x(\tau) d\tau \quad (2)$$

where the kernel function $\omega_{\alpha}(t)$ satisfies the following three conditions:

$$\begin{aligned} \omega_{\alpha}(t) &= 0, \quad \text{if } |t| = \alpha \\ \int_R \omega_{\alpha}(t) dt &= 1 \end{aligned} \quad (3)$$

$\omega_{\alpha}(t)$ has n continuous derivatives.

The piece-wise polynomial kernels described in Aksyonova and Shelekhova (1995) were used for derivative estimation. This type of kernel allows the

fast derivative estimation, which is important for on-line applications of the algorithm.

The detection of the occurrence of a spike was determined by a threshold crossing algorithm applied to the derivative of the signal instead of the raw signal. This allowed using the filtering feature of the operator during derivative estimation. The regularization parameter α corresponds to the time interval that is used for signal smoothing and for calculation of its derivatives. The integral operators act as band-pass filters on the signal such that transfer characteristics can be calculated. Low and high cutoff frequencies are inversely proportional to parameter α of Eq. (2). For the first derivative: $\omega_{\text{low}} \approx 0.8/\alpha$, $\omega_{\text{high}} \approx 4.76/\alpha$ and for the second derivative: $\omega_{\text{low}} \approx 1.76/\alpha$, $\omega_{\text{high}} \approx 5.44/\alpha$. The neuronal spike durations range from 0.5 to 4 ms, i.e. with frequencies ranging from 2 to 0.25 kHz, respectively. The value of the parameter α was chosen in order to optimize detection of signals with frequencies near 1.0 ± 0.5 kHz.

The third-order equation of the form $\frac{d^3x}{dt^3} = f^*\left(\frac{dx}{dt}, \frac{d^2x}{dt^2}\right)$ was used in our algorithm. First and second derivatives, and not the signal itself, were used with the selected regularization parameter for filtering purposes. We noticed that increasing the order of the equation to fourth-order and beyond did not provide a significant enhancement of the results but increased the calculation time.

2.2.2. Unsupervised iterative learning procedure

An unsupervised learning algorithm for spike sorting is necessary in order to provide a fast and user-friendly selection tool to use during a real-time experiment or during human neurosurgery. We have developed an unsupervised iterative learning algorithm that estimates the number of classes and their centers according to the Euclidian distance between spike trajectories in phase space.

The traditional approach to construct templates for classes is to estimate the mean trajectory of the cluster. However, the estimation of the mean is not robust to outliers that unavoidably appear in the learning set collected without user supervision, in presence of noise and artefacts. Instead of averaging the observed trajectories to estimate the mean, our algorithm selects one of them to be considered as a template representing a class. To evaluate this trajectory the algorithm analyzes the learning set in order to find the trajectories with

maximal probability density in their neighborhood. The rationale is that in case of a Gaussian distribution the mean corresponds to the maximum of the probability density. The distribution of the squared distances from the center to all other spikes belonging to a given class was used to estimate the class radius. The square of the distance from each spike to the center of its class follows a χ^2 distribution, because vectors of trajectories normal deviation in phase space are normally distributed.

2.2.3. On-line classification

After the unsupervised learning procedure, the classification of the signals for the spike sorting can be performed according to the minimal Euclidian distance in phase space between the actual spike trajectory and the centers of the templates classes. The classification implemented on the platform Macintosh PowerPC G4 400 MHz is fast enough to be used in real-time application.

2.3. USS software implementation

A cross-platform USS software was developed with three blocks: Data Acquisition Block, Calculation Modules and User Interface. The Calculation Modules are developed using C++ programming language. Their code can be compiled by Microsoft Visual Studio 6.0 (Microsoft Corp., Redmont, WA) running on Microsoft Windows 2000/XP (Microsoft Corp., Redmont, WA) operating system and compiled as dynamic libraries by CodeWarrior (Metrowerks, Austin, TX) for Macintosh (Apple Computer Inc., Cupertino, CA) platforms with MacOS 9.x (Apple Computer Inc., Cupertino, CA) operating system. The user Interface was developed and compiled with LabView 6.0 (National Instruments, Austin, TX). The USS software allows on-line spike sorting with minimal interactions with user. The output files corresponding to the spike trains are in standard ASCII format for multivariate time series, originally proposed by Professor Moshe Abeles at the Department of Neurophysiology of the Hebrew University, Jerusalem.

The software allows off-line analysis of pre-recorded data. Analog files corresponding to the electrophysiological signals in standard formats like WAV and AIFF, as well as customized formats with defined sampling rates and bits resolution, are readable by the

program. The Calculation Modules process the data stream independently of the data source. The program offers three operating modes to the user: signal visualization without any processing, learning set collection and classification. The data stream is recorded in a buffer and the buffer is processed according to the operating mode. The signal visualization operating mode displays the raw signal and the first order derivative. This visual inspection can be useful to the user for modifying the default values of the level of spike detection threshold and regularization parameter for the derivative calculations. The user can determine whether the learning phase starts after a minimum interval of acquisition or after a minimum number of suprathreshold events has been collected. For a learning set of 300 spikes the learning process takes about 10–15 s on a personal computer equipped with a Pentium3 500 MHz (Intel Corp., Santa Clara, CA) and about 6–8 s on a Macintosh PowerPC G4 400 MHz (Apple Computer Inc., Cupertino, CA).

The iterative learning procedure used in USS mentioned above converges to the local maximums of probability density not always corresponding to classes. From over side several branches of the algorithm started from different initial point may converge to different points in the local maximum vicinity. So not all the templates represent a cluster and several templates may represent one class. Some post processing of the results of the learning was added. First of all we eliminate overlapping classes. Classes are formed by all the spike trajectories in R -vicinity of the template trajectory. If more than p percents of the trajectories of one class belong also to another class, the both classes are considered to represent the same neuron with high probability and the less representative class is eliminated. By default $p = 80\%$; user is allowed to change this parameter. Some low amplitude classes may appear due to background noise and non-representative classes due to artifacts. To eliminate them automatically we used the criteriom $(a/A) \times (n/N) < k$, where a is the amplitude of the class template, A is the maximal template amplitude, n is the number of class members, N is the learning dataset volume, k is a parameter. The parameter k is by default equal 0.12; this value can be changed by user.

Nevertheless, the implementation of the learning in USS is semiautomatic. After the post-processing the results are displayed that offers to user the possibility to

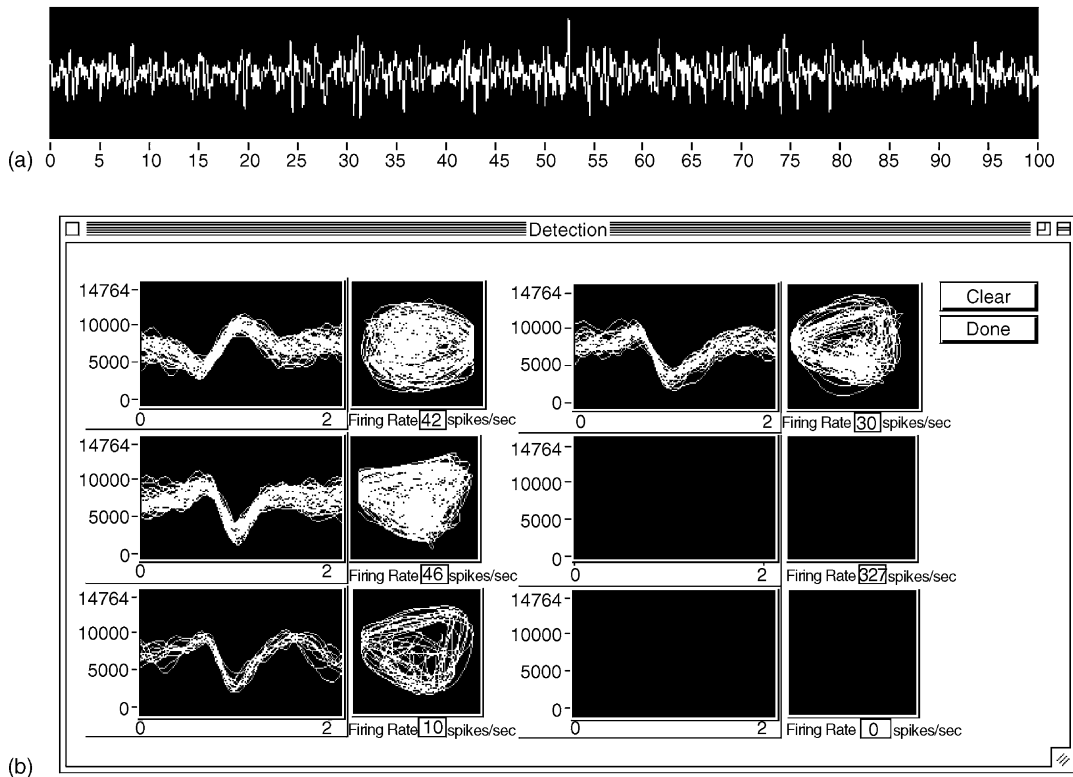


Fig. 1. (a) A 100 ms fragment of a real signal. (b) The classification window displays the classified events while the classification process. For each class the time domain (here with a window duration of 2 ms and arbitrary units for the spike amplitude) and phase space spike trajectories are shown. For each class the current firing rate is indicated as well. Here the classification process for the one electrode real signal (a) represented.

select only specific classes. All the information about selected templates is saved into a file, such that the templates could be loaded for later usage and applied to other records. After the selection of the templates the program is ready to perform the on-line classification of spikes. The suprathreshold events are either classified in one of the selected classes and displayed in a classification window (Fig. 1(b)) or in a “generic” class. The epochs of the events of all classes, but the “generic” class, are recorded as a multivariate time series. By default the time resolution of the time series is set to 1 ms.

2.4. Test files

Analog recordings distributed by Alpha-Omega Inc. (Nazareth, Israel) corresponding to a mixture of three single units discharges were digitized at a 50 kHz sam-

pling rate and used as raw files. USS was applied to these recordings and extracted three spike templates (Fig. 2(a)). Test files were obtained by random insertion of these three templates in files with different levels of background noise. The noise was extracted from the electrophysiological recordings performed in the STN during surgery on a Parkinsonian patient at the University Hospital of Grenoble. Two levels of signal-to-noise ratio were used for testing: JR SNR of 2.5 dB and 3.55 dB. For each level of noise classification scores of USS were computed for two sets of data. The first set is the test file without pre-processing, while the second set is the test file processed with a TSA denoising procedure before undergoing USS analysis. The TSA denoising procedure is a wavelet based technique that has been originally proposed for denoising speech signals (Bahoura and Rouat, 2001). It is based on the principle of time and spatial adaptive thresholding of

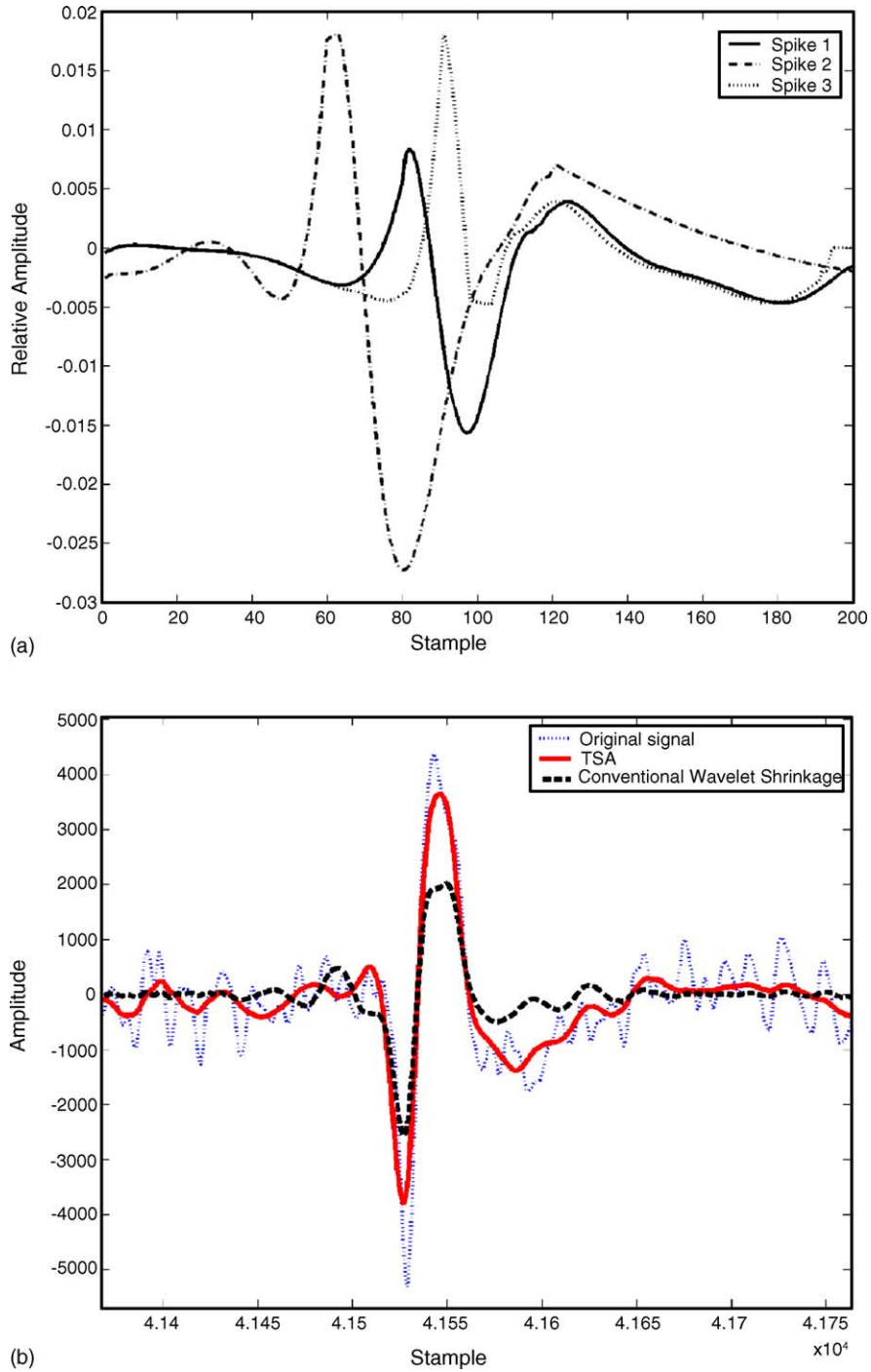


Fig. 2. (a) Three templates used for testing. (b) Comparison of deformations introduced by TSA and conventional wavelet thresholding denoising algorithms.

the wavelet coefficients. TSA was selected for the tests because it does not require an explicit estimation of the noise level nor of the a priori knowledge of the SNR, which is usually needed in most of the popular enhancement methods. The originality of TSA resides in its ability to modulate in time and scale the wavelet thresholds depending on the noise and on the signal time evolution.

2.5. Data files

The electrophysiological data were collected from six Parkinsonian patients, mostly suffering from severe akinesia with disabling motor fluctuation and rigidity, and for some of them, from tremors. Surgical operation for chronic deep brain stimulation of STN was performed under local anesthesia at the department of neurosurgery of the University Hospital of Grenoble (Benabid et al., 2002). Pharmacological PD medication was stopped 12 h before surgery. Patients were placed in a stereotaxic frame and bilateral STN were targeted. The location of each STN was determined using ventriculography landmarks, i.e. midline of the third ventricle and the anterior (AC) and posterior (PC) commissures. The antero-posterior coordinates of STN were calculated according to a proportional scheme based on the AC-PC line and the lateral coordinates were set at 12 mm from the middle of the third ventricle. A surgical microdrive allowing five simultaneous parallel trajectories, with four around each 2 mm apart from the central one, was used. Tungsten bipolar microelectrodes (Frederick Haer and Co., Brunswick, ME), with impedances ranging from 0.1 to 0.6 M Ω (at 1 kHz) were used for recording neuronal activity. Recordings were performed at different sites along the trajectory, using the Neurotek System (AlphaOmega, Nazareth, Israel) which comprises five isolated preamplifiers that provide five simultaneous recordings. The recordings were saved in digital format for off-line analysis by USS.

At the end of the recording sessions, electrical stimulation was applied every 2 mm along the trajectory to assess the clinical effect of the stimulation and to determine the threshold of side effects. On the basis of this clinical assessment and of the electrophysiological recordings the surgical team selected the most appropriate site for the chronic implantation of the stimulating macroelectrode. During and in the end of the

surgical procedure, a teleradiological X-ray control allowed for identification of the position of the tip of each micro-electrode. Five days after surgery, an MRI examination was performed using T1-weighted images in a 1.5 T Philips Gyroscan in order to assess the final position of the tip of the macroelectrode (Medtronic 3389, Minneapolis, USA) within the STN and the lack of bleeding around it.

3. Results

3.1. Evaluation of USS performance

A raw file formed by 1003 events was generated after introducing three template spikes at random times. Two levels of additional noise (SNR = 2.5 dB, SNR = 3.55 dB) were superimposed to the raw file in order to obtain two test files. The test files were also tested after pre-processing by a TSA denoising procedure described above. The performance of USS with different test files was determined according to two types of errors due to an incorrect classification. The first type of error is due to “false alarms”, that means the detection of events that were absent in the original unprocessed file. The rate of false alarms can be computed exactly as we know the exact epochs of all spikes in the test file without noise and without applying denoising pre-processing. The second type of error is defined as “non-detection”, which corresponds to missing the detection of an event present in the original unprocessed file.

The comparison of USS performance without any noise and with a background noise typical for real data recordings in the surgery room (SNR = 2.5 dB) showed that about 8% of spike occurrences were missed but no misclassification was observed (Table 1). The application of TSA wavelet based technique for denoising did not improve USS performance. With or without pre-processing the number of false alarms generated by USS is very low (equal to 0 for for SNR of 3.5 dB and 1.5% for recording conditions close to that of the surgery room). Conversely, denoising increased the error due to missed detection up to nearly 17% (Table 1). Spikes are missed randomly and the distribution inside the classes is not modified by this error. On the opposite, a large impact of false alarms could affect significantly the distribution of the events among the different classes.

Table 1
Error rate of USS tested on a sample file of 1003 events distributed into three classes

	Original signal	SNR 2.5 dB	SNR 3.55 dB	SNR 3.55 dB with TSA
Misclassification	0	0	0	0
False alarm	0	1%	0	0
Non-detection	0	8%	3%	10%
Total	0	10%	3%	10%

The error rate is shown without additive noise, with two levels of signal-to-noise ratio (SNR) and with TSA denoising procedure.

This error would create an incorrect evaluation of the relative frequency of the events per time unit. We also tested the approach with conventional wavelet thresholding (Donoho and Johnstone, 1994) and the results that we obtained were even worse than by applying TSA. In fact, conventional wavelet shrinkage enhancement techniques do not adapt the threshold following the signal and introduce more distortions into the signal itself (Fig. 2(b)).

3.2. Time domain analysis of spike trains

The data sample was formed by multi-unit recordings collected at 49 recording sites in six Parkinsonian patients. At each recording site five channels were recording simultaneously the bioelectric activity from five microelectrodes. We could analyze 127 single channel recordings characterized by steady-state recording conditions out of a maximum number of 245. The level of the threshold for the spike detection was set, by default, equal to 2.5 times the variance of the signal derivative in order to exclude most of the noise that could interfere with template identification. An overall amount of 492 single unit spike trains could be sorted out from the multi-unit recordings.

Time domain analyses included autocorrelations ($n = 492$) for each spike train. Crosscorrelations ($n = 831$) were calculated for pairs of units recorded from the same microelectrode. These computations were performed with the software DAN accessible on public domain at the website <http://dan.unil.ch>. Bursting and synchronized activity patterns were detected according to the parameters described in (Villa and Lorenzana, 1997). It is worth reporting that bursts of discharges were considered as such only if their average duration was longer than 10 ms (Fig. 3(a)). All the analysis were carried out separately for the initially operated side (side I) and the second operated side (side II). The results of time domain analyses (Table

2) show that the percentage of bursting cells was comprised on average between 5 and 20%, with a tendency to be more abundant in the first operated side, even though this difference was not statistically significant (t -test, $2P = 0.19$). Crosscorrelograms characterized by a hump near zero lag indicate that both single units tend to fire in synchrony (Fig. 3(b)). The percentage of STN pairs of units firing synchronously was near 20% on average but this ratio could be as high as 60%, as observed in one hemisphere of patient $n. 2$.

3.3. Frequency domain analysis of spike trains

The analysis of the autocorrelations clearly showed highly distinctive oscillatory patterns of different frequencies (Fig. 4). Notice that the multi-unit channel recordings defined during surgery as “tremor cells” always allow the sorting of a spike train with characteristic oscillation frequency components at about 4–6 Hz (Fig. 4(a)). For each single-unit time series we calculated the power spectrum by applying the Fast Fourier Transform to the autocorrelogram trace with an epoch equal to 2000 ms.

The significant peaks of the power spectrum were detected assuming that the neuronal firing is a Poissinian process and the confidential level is equal to 0.99 (Fig. 4(b and d)). The sum of all occurrences of power spectrum threshold crossings were computed for each frequency value in the range [1,50] Hz for side 1 and side 2 separately (Fig. 5). We assumed that these values followed a distribution with heavy tails. Then we estimated the variance of this normal distribution with the method of maximum likelihood.

This calculation was performed as follows. The spectral analysis was performed in the frequency range [0–50] Hz by steps of 1 Hz. Let be $a(\omega)$, $\omega = 1, \dots, 50$ the number of threshold crossings for each frequency in the range of interest. For a Poisson random process we have a series with $p = 0.01$ probability of

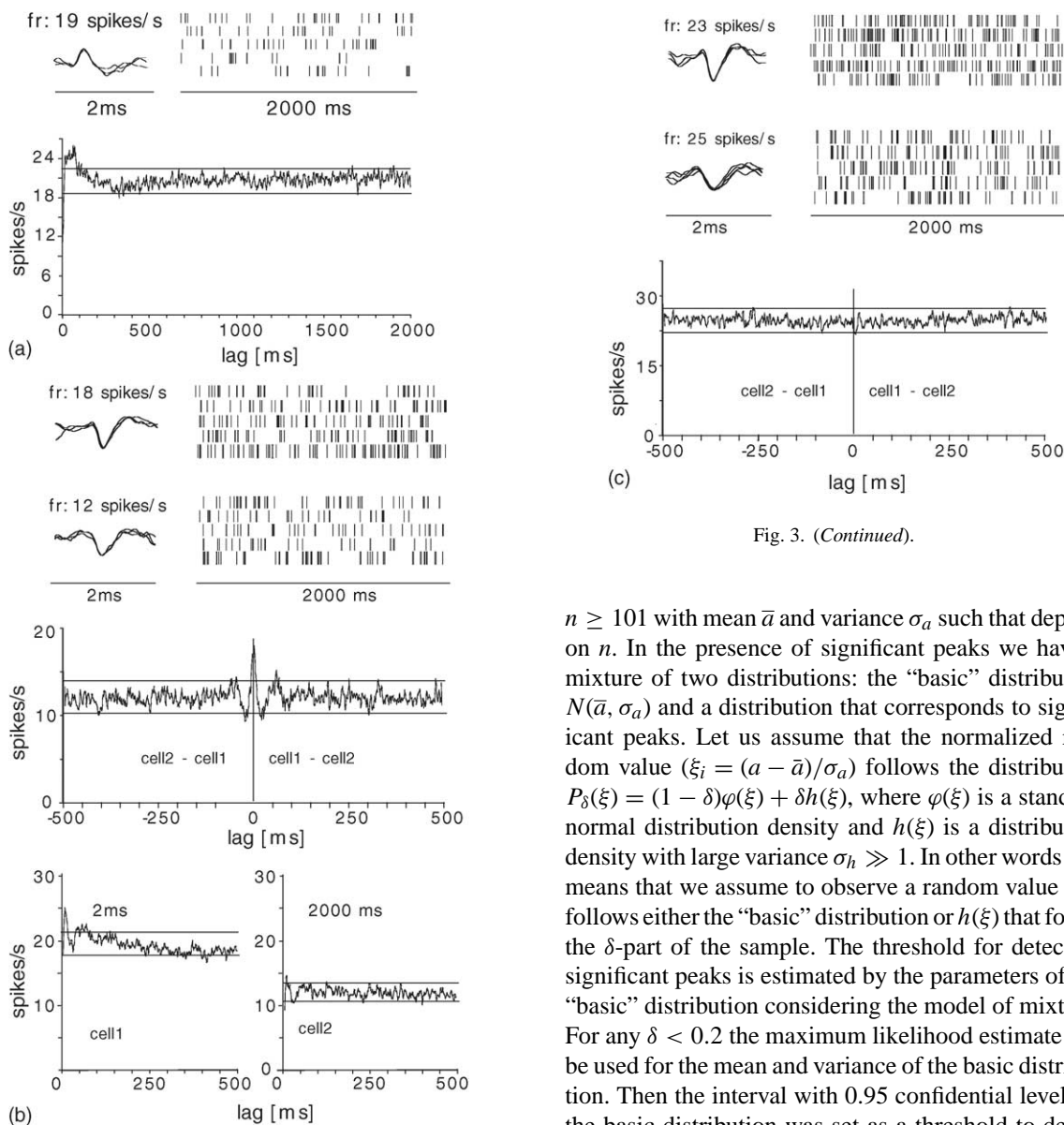


Fig. 3. (Continued).

Fig. 3. (a) Autocorelogram of a bursting cell, (b) cross- and autocorrelograms of two synchronized cells and (c) cross- and autocorrelograms of two unsynchronized cells. The abscissa represents a lag in ms and the ordinate-firing rate in spikes/s. The horizontal lines represent confidential levels.

threshold crossing for each $a(\omega)$. Binomial distribution can be approached by normal distribution for the number of observation determined by $np(1 - p) \geq 9$. Thus, $a(\omega)$ can be considered as normal distributed if

$n \geq 101$ with mean \bar{a} and variance σ_a such that depend on n . In the presence of significant peaks we have a mixture of two distributions: the “basic” distribution $N(\bar{a}, \sigma_a)$ and a distribution that corresponds to significant peaks. Let us assume that the normalized random value ($\xi_i = (a - \bar{a})/\sigma_a$) follows the distribution $P_\delta(\xi) = (1 - \delta)\varphi(\xi) + \delta h(\xi)$, where $\varphi(\xi)$ is a standard normal distribution density and $h(\xi)$ is a distribution density with large variance $\sigma_h \gg 1$. In other words this means that we assume to observe a random value that follows either the “basic” distribution or $h(\xi)$ that forms the δ -part of the sample. The threshold for detecting significant peaks is estimated by the parameters of the “basic” distribution considering the model of mixture. For any $\delta < 0.2$ the maximum likelihood estimate can be used for the mean and variance of the basic distribution. Then the interval with 0.95 confidential level for the basic distribution was set as a threshold to detect the significant peaks in the power spectrum.

We used a threshold corresponding to the confidential level 0.95 estimated for the side 1 to define the frequency bands with high probability density and considered as clusters the areas where the curve from (Fig. 5) is above the threshold line. Three frequency bands were defined: [0–2] Hz, [4–6] Hz, [8–10] Hz (Fig. 5). The frequency bands [0–2] Hz [4–6] Hz tend to be more representative on the first operated side (Table 2). However, the only statistically significant difference

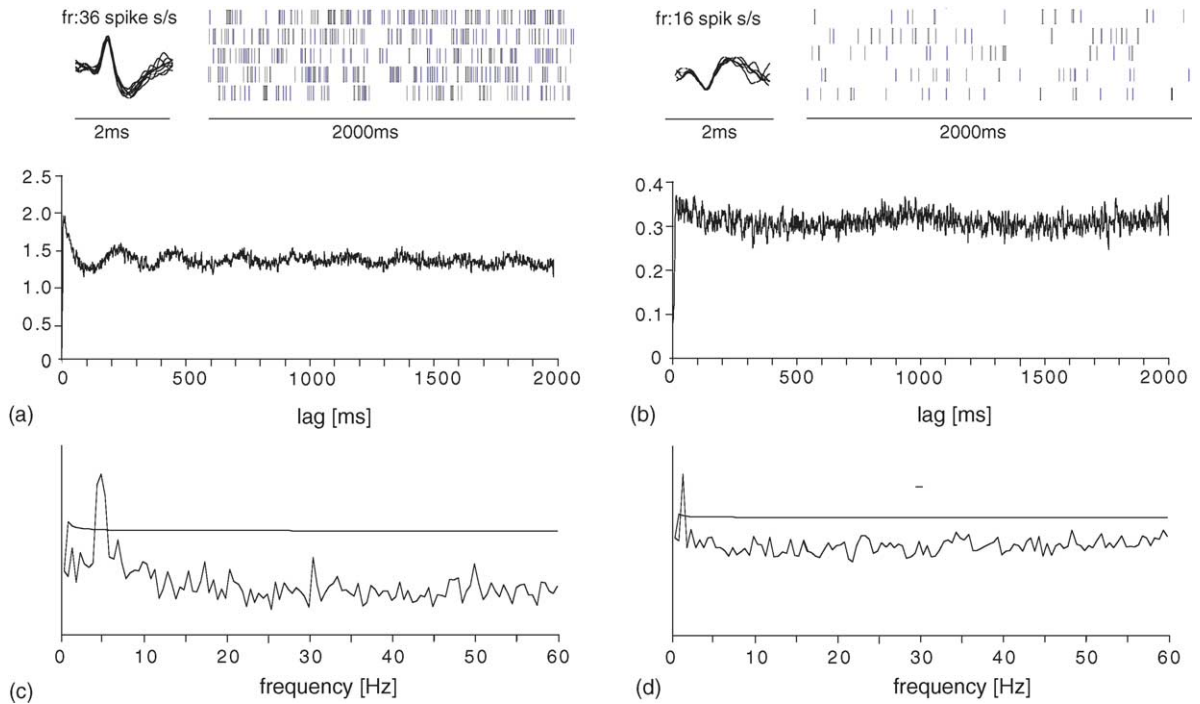


Fig. 4. Two single units characterized by an oscillatory firing pattern. Autocorrelograms (a and c) and power spectrum (b and d) of the first and second unit, respectively. Notice the first unit (left panel) is characterized by oscillation rates ~ 5 Hz, while the second cell (right panel) is characterized by low-frequency oscillations ~ 1 Hz.

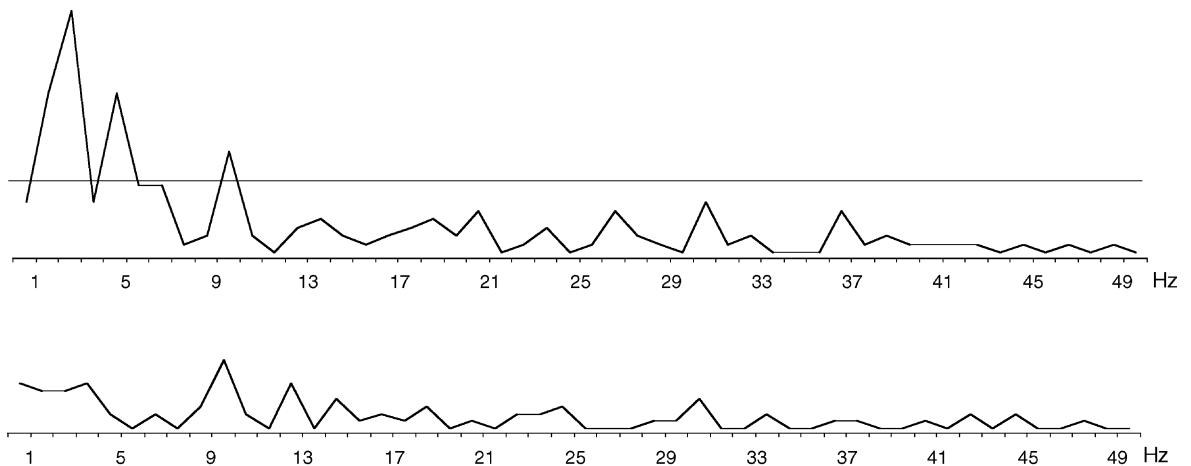


Fig. 5. Cumulated distribution of significant peaks detected in the spectrum of single units characterized by oscillatory patterns. All occurrences of significant peaks in the frequency range [0–50] Hz were added together for side I (upper panel) and side II (lower panel). The curves represent the probabilities of occurrence of the peaks at a resolution of 1 Hz. The horizontal line represents a 95% level of significance. The following clusters appeared: [0–2] Hz, [4–6] Hz, [8–10] Hz.

Table 2
Percentages of bursting, synchronized, and oscillatory firing patterns for six patients

Patient	Side	Cellcount	Paircount	Synchronization	Bursting	Oscillation [0–2] Hz	Oscillation [4–6] Hz	Oscillation [8–10] Hz
1	I	34	62	23	35	35	9	3
	II	23	47	6	9	4	0	0
2	I	11	25	44	18	27	0	0
	II	30	47	44	0	3	0	34
3	I	39	46	13	23	23	20	0
	II	23	44	29	9	0	0	0
4	I	33	62	13	12	6	3	6
	II	37	81	14	3	5	0	0
5	I	77	118	21	26	20	17	12
	II	57	94	12	18	9	4	5
6	I	49	69	13	10	12	6	2
	II	79	136	6	3	3	3	5
Total	I	243	382	19	21	19	11	6
	II	249	449	15	7	4	2	3

Side I corresponds to the first operated hemisphere.

between the two operated sides was observed for the frequency band [0–2] Hz (*t*-test, $2P = 0.028$).

4. Discussion

This paper has presented new results about the performance of a method for unsupervised spike sorting (USS) recently developed (Aksenova et al., 2003). The USS algorithm demonstrated its performance in separating single units signals with an amplitude beary greater than the amplitude of background noise. A denoising procedure such as TSA, very efficient for improving the recognition of speech signals in a noisy environment (Bahoura and Rouat, 2001), could not improve at all, even worsened, the performance of USS. This result was rather surprising but can be understood as the TSA denoising should also be applied to the prototype's shape. These results suggest that TSA modifies spatiotemporal cues of the signal that are used by the USS procedure to perform the spike sorting. In order to increase the performance, a pre-processing by TSA

of the spike templates should also be applied. This approach may be explored in the future with other denoising procedures, but the performance obtained by USS with SNR as low as 2.5 dB provides evidence that USS may be used for medical application with considerable confidence.

Electrophysiological recordings performed in six Parkinsonian patients undergoing neurosurgical intervention for the implantation of chronic electrodes in STN were analyzed by USS. Five channels recordings were performed simultaneously during the operation. Each single channel recording was characterized by multi-unit activity. This information is not suitable for analyzing temporal firing patterns as it may be blurred by the summation of several single unit activities characterized by different discharge patterns. The application of USS let us sort up to eight single units from one channel although the average was 3–4 single units sorted out from one multi-unit recording. The analysis of single unit firing pattern may reveal interesting functional features related to the region of interest which is examined by the microelectrodes. We analyzed 492 sin-

gle units recorded in the STN that could be classified into several classes according to their firing pattern. Synchronized activity was observed in about 20% of the pairs of units recorded from the same electrode.

The two main classes of firing patterns were formed by cells characterized by bursting and by oscillatory components. Bursting was observed in about 20% of the cells, a ratio similar to the synchronized firing pattern. In our previous animal study performed in the substantia nigra pars reticulata (SNpr) we observed that an increase in synchronous firing could be associated with an increased tendency to fire in bursts with pharmacological modulation of glutamatergic activity (Villa and Lorenzana, 1997). The data reported here refer to STN, which is the main glutamatergic nucleus of the basal ganglia, and the present finding could indicate that the relation between bursting and synchronized activity might be a general feature of the mammalian basal ganglia.

Oscillatory patterns were further classified according to the main frequency component. The activity patterns observed in the first operated side indicate a rather large proportion (19%) of very low frequency components. In the second operated side these components were observed in a very minority of the cells (about 4%) (Table 2). This observation might suggest that these components are somewhat related to the state of arousal of the patient and carry no valuable information with respect to the patterns of firing of Parkinsonian patients.

An alternative explanation of the difference between the two hemispheres could be that the intervention into one hemisphere affects the neuronal activity in the second one. Low-frequency oscillations in the range [0–2] Hz were suggested as a resonant frequency generated by the feedback system formed by the excitatory STN and the inhibitory external globus pallidus (Plenz and Kitai, 1999). The stimulations performed in the first operated hemisphere might provoke changes of neuronal activity in the second hemisphere. This possibility can not be discarded but the electrical stimulation performed during surgery is applied for short periods of time, necessary to assess the acute remission of neurological symptoms. Such acute stimulation does not seem to account for a long-term change in the other hemisphere if one considers that several hours may separate the recordings performed in the two hemispheres. This observation has led us to investigate whether a difference between the two hemispheres

could be observed in other neurosurgical operations that involve bilateral implantation of macroelectrodes for DBS, such as chronic implantation of electrodes in the globus pallidus of dystonic patients. This investigation is currently in progress at the University Hospital of Grenoble.

References

- Abe, K., Asai, Y., Matsuo, Y., Nomura, T., Sato, S., Inoue, S., Mizukura, I., Sakoda, S., 2003. Classifying lower limb dynamics in Parkinson's disease. *Brain Res. Bull.* 61, 219–226.
- Aksenova, T., Chibirova, O., Benabid, A.-L., Villa, A., 2002. Nonlinear oscillation models for spike separation. *Lecture Notes Comput. Sci.* 2526, 61–70.
- Aksenova, T., Chibirova, O., Dryga, A., Tetko, I., Benabid, A.-L., Villa, A., 2003. An unsupervised automatic method for sorting neuronal spike waveforms in awake and freely moving animals. *Methods, A Companion Methods Enzymol.* 30, 178–187.
- Aksyonova, T.I., Shelekhova, V.Y., 1995. Efficient algorithms of derivative estimation for noisy observations. *SAMS* 18, 159–163.
- Asai, Y., Nomura, T., Sato, S., Tamaki, A., Matsuo, Y., Mizukura, I., Abe, K., 2003. A coupled oscillator model of disordered interlimb coordination in patients with Parkinson's disease. *Biol. Cybern.* 88, 152–162.
- Bahoura, M., Rouat, J., 2001. A new approach for wavelet speech enhancement. *IEEE Signal Process. Lett.* 8 (1), 10–12.
- Benabid, A.-L., Koudsie, A., Benazzouz, A., Pollak, P., 2002. Imaging of subthalamic nucleus and ventralis intermedius of the thalamus. *Movement Disord.* 17, 123–129.
- Benabid, A.-L., Pollak, P., Gross, C., Hoffmann, D., Benazzouz, A., Gao, D.M., Laurent, A., Gentil, M., Perret, J., 1994. Acute and long-term effects of subthalamic nucleus stimulation in parkinson's disease. *Stereotactic Func. Neurosurg.* 62, 76–84.
- Benazzouz, A., Gao, D.M., Ni, Z.G., Piallat, B., Bouali-Benazzouz, R., Benabid, A.-L., 2000. Effect of high-frequency stimulation of the subthalamic nucleus on the neuronal activities of the substantia nigra pars reticulata and ventrolateral nucleus of the thalamus in the rat. *Neuroscience* 99, 289–295.
- Bergman, H., DeLong, M.R., 1992. A personal computer-based spike detector and sorter: implementation and evaluation. *J. Neurosci. Methods* 41, 187–197.
- Bevan, M.D., Magill, P.J., Terman, D., Bolam, J.P., Wilson, C.J., 2002. Move to the rhythm: oscillation in the subthalamic nucleus-external globus pallidus network. *Trends Neurosci.* 25, 525–531.
- Cassidy, M., Mazzone, P., Oliviero, A., Insola, A., Tonali, P., Lazzaro, V.D., Brown, P., 2002. Movement-related changes in synchronization in the human basal ganglia. *Brain* 125, 1235–1246.
- Donoho, D.L., Johnstone, I.M., 1994. Ideal spatial adaptation by wavelet shrinkage. *Biometrika* 81 (3), 425–455.
- Fee, M.S., Mitra, M., Klenfeld, D., 1996. Variability of extracellular spike waveforms of cortical neurons. *J. Neurophysiol.* 76, 6.

- Forster, C., Handwerker, H., 1995. Automatic classification and analysis of microneurographic spike data using a PC/AT. *J. Neurosci. Methods* 31, 109–118.
- Gadikie, R., Albus, K., 1995. Real-time separation of muktineuron recordings with a DSP32C signal processor. *J. Neurosci. Methods* 57, 187–193.
- Gudzenko, L.I., 1962. The statistical method of determination of characteristics of a non-control autooscillating system. *Izvestiia Vuzov Radiophysics* 5, 572–587 (in Russian).
- Hashimoto, T., Elder, C.M., Okun, M.S., Patrick, S.K., Vitek, J.L., 2003. Stimulation of the subthalamic nucleus changes the firing rate pattern of pallidal neurons. *J. Neurosci.* 23, 1916–1923.
- Hurtado, J.M., Gray, C.M., Tamas, L.B., Sigvardt, K.A., 1999. Dynamic of tremor related oscillation in the human globus pallidus: a single case study. *Proc. Natl. Acad. Sci. U.S.A.* 16, 1674–1679.
- Hutchison, W.D., Lozano, A.M., Tasker, R.R., Lang, A.E., Dostrovsky, J.O., 1997. Identification and characterization of neurons with tremor-frequency activity in human globus pallidus. *Exp. Brain Res.* 113, 557–563.
- Levy, R., Ashby, P., Hutchison, W.D., Lang, A.E., Lozano, A.M., Dostrovsky, J.O., 2002. Dependence of subthalamic nucleus oscillations on movement and dopamine in Parkinson's Disease. *Brain* 125, 1196–1209.
- Levy, R., Hutchison, W.D., Lozano, A.M., Dostrovsky, J.O., 2000. High-frequency synchronization of neuronal activity in the subthalamic nucleus of parkinsonian patients with limb tremor. *J. Neurosci.* 20, 7766–7775.
- Levy, R., Hutchison, W.D., Lozano, A.M., Dostrovsky, J.O., 2002. Synchronized neuronal discharge in basal ganglia of parkinsonian patients in limited oscillatory activity. *J. Neurosci.* 22, 2855–2861.
- Lewicki, M.S., 1998. A review of methods for spike sorting: the detection and classification of neural action potentials. *Network Comput. Neural Syst.* 9, 53–78.
- Limousin, P., Krack, P., Pollak, P., Benazzouz, A., Ardouin, C., Hoffmann, D., Benabid, A.-L., 1998. Electrical stimulation of the subthalamic nucleus in advanced parkinson's disease. *N. Engl. J. Med.* 339, 1105–1111.
- Liu, X., Ford-Dunn, H.L., Hayward, G.N., Nandi, D., Miall, R.C., Aziz, T.Z., Stein, J.F., 2002. The oscillatory activity in the parkinsonian subthalamic nucleus investigated using the macro-electrodes for deep brain stimulation. *Clin. Neurophysiol.* 113, 1667–1672.
- Magarinos-Ascone, C.M., Figueras-Mendez, R., Riva-Meana, C., Cordoba-Fernandez, A., 2000. Subthalamic neuron activity related to tremor and movement in Parkinson's disease. *Eur. J. Neurosci.* 12, 2597–2607.
- Niktarash, A.H., 2003. Transmission of the subthalamic nucleus oscillatory activity to the cortex: a computational approach. *J. Comput. Neurosci.* 15, 223–232.
- Plenz, D., Kitai, S.T., 1999. A basal ganglia pacemaker formed by the subthalamic nucleus and external globus pallidus. *Nature* 400, 677–682.
- Rodrigues, M.C., Guiridi, O.J., Alvarez, L., Mewes, K., Macias, R., Vitek, J., DeLong, M.R., Obeso, J., 1998. The subthalamic nucleus and tremor in Parkinson's disease. *Movement Disord.* 13 (Suppl.), 111–118.
- Schmidt, E.M., 1984. Computer separation of multi-unit neuroelectric data: a review. *J. Neurosci. Methods* 12, 95–111.
- Villa, A.E.P., Lorenzana, V.M.B., 1997. Ketamine modulation of the temporal pattern of discharges and spike train interactions in the rat substantia nigra pars reticulata. *Brain Res. Bull.* 43, 525–535.